QCD structure of quarkonium spin spectra

F. Halzen, C. Olson, M. G. Olsson, and M. L. Stong
Department of Physics, University of Wisconsin, Madison, Wisconsin 53706
(Received 25 June 1992; revised manuscript received 23 December 1992)

We show that our QCD calculation of the $^1P_1$ charmonium state can be incorporated into a global description of the fine and hyperfine structure of the charmonium and bottomonium systems. We propose a simple renormalization prescription in which all ambiguities are absorbed into a single strong coupling constant α_s. We find that the $O(\alpha_s^2)$ perturbative QCD potential leads to a consistent description of all splittings. The results are used to predict the unmeasured bottomonium P-wave hyperfine splittings.

PACS number(s): 14.40.Gx; 12.38.Bx; 12.40.Qq

In an earlier paper [1] we demonstrated that the hyperfine splittings of P-wave states in heavy quarkonia can be reliably calculated via perturbative QCD and are consistent with experimental indications [2]. The angular dependence of the wave functions and of the potential is such that the calculation is independent at the one-loop level of renormalization scheme and scale, leaving the splitting a function of only the quark mass and α_s. This independence, and therefore predictive power, does not occur in the calculation of either S-wave hyperfine splittings or the P-wave spin-orbit and tensor splittings. A single choice of the renormalization scale may be made for each quark mass, and despite the uncertainties in the calculation of these splittings, our previous perturbative QCD calculation can be generalized to all spin splittings with results consistent with experiment.

This differs from previous calculations of the same quantities in the greatly simplified approach to renormalization scheme and correspondingly to α_s. Other authors have fixed μ and α_s using the Grunberg [3] prescription and the experimental data for each state [4], or by minimizing the effect of higher-order terms generated

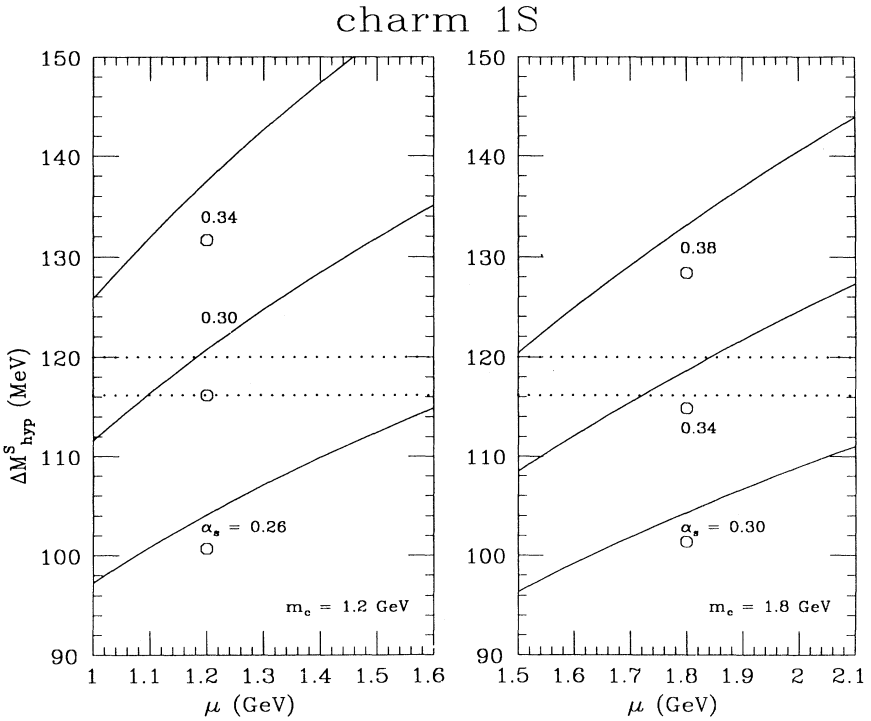

FIG. 1. Hyperfine splitting, $\Delta M^S_{\rm hyp} = M(J/\Psi) - M(\eta_c)$, in the charmonium $1S$ system, for three values of α_s. The large circles give the tree-level results for the same values of α_s. They have been placed at $\mu = m_c$ to demonstrate that the one-loop corrections are small for this choice of μ. The dotted horizontal lines indicate the experimental $1\,\sigma$ limits.

 ©1993 The American Physical Society

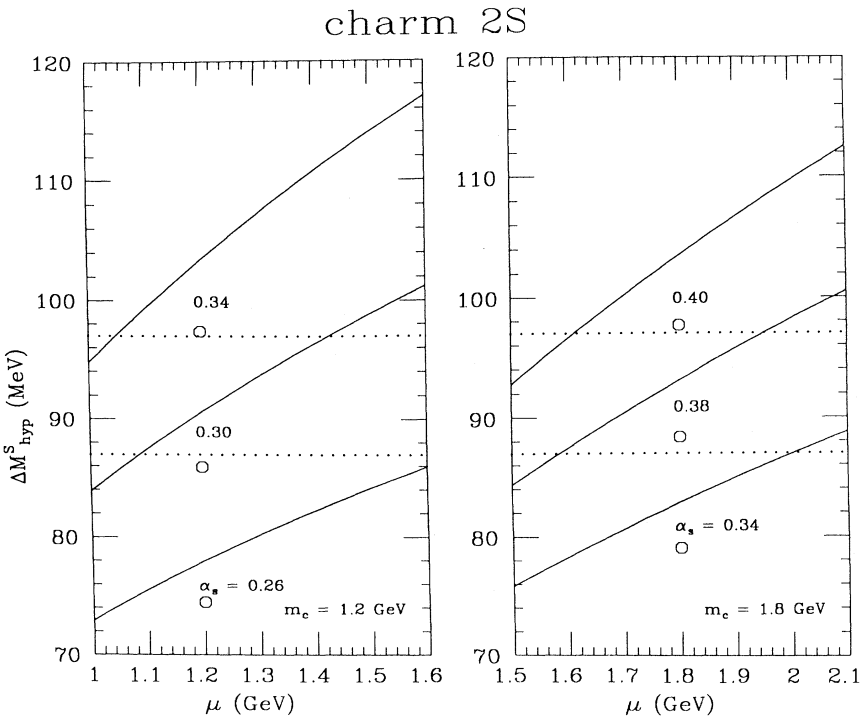

FIG. 2. Similar to Fig. 1, for the charmonium $2S$ states. Notice that the three values of α_s have changed for $m_c = 1.8$ GeV.

by renormalization-group improvement of the potential [5]. One disadvantage of the first approach is that this scheme allows each state to have a different value of μ and hence of α_s. It is also unclear how the Grunberg prescription is to be implemented in such a case as the hyperfine P-wave splittings, which are zero at the tree level. The fine-structure splittings cause additional difficulties, as they then require a very large α_s yet only small higher-order corrections.

Section I introduces the wave functions and the perturbative QCD calculation, Sec. II presents results for the hyperfine splittings in charmonium, and Sec. III discusses the spin-orbit and tensor calculations. We conclude with predictions for the P-wave hyperfine splittings in bottomonium.

I. CALCULATION SCHEME

For a given charm-quark mass we fit to the spin-averaged charm and bottom spectra to obtain the corresponding potential parameters and bottom-quark mass. We perform our calculation with two choices of m_c: 1.2 GeV and 1.8 GeV. Because the fitting process fixes m_b the lower (higher) charm-quark mass implies a lower (higher) bottom-quark mass. It is possible to use the spin-averaged spectra to fit the charm-quark mass; we prefer to retain two values in order to understand the effect of m_q on our results. This point has been overlooked

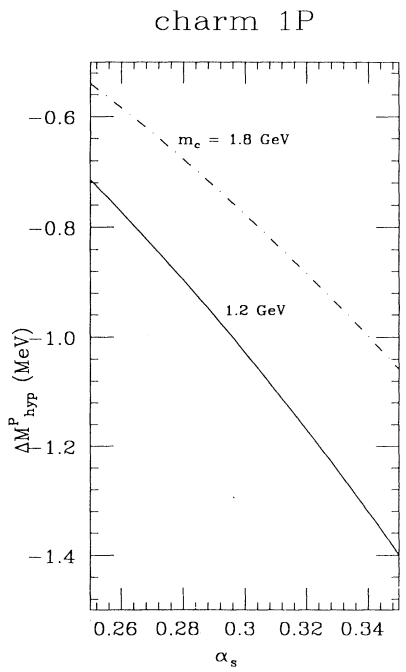

FIG. 3. ΔM^P_{hyp} in charmonium $1P$. The result is independent of μ. $\alpha_s = 0.3$ gives splittings of -1.0 and -0.78 MeV for $m_c = 1.2$ and 1.8 GeV, respectively.

in earlier treatments of the subject [4–7]. We treat the spin splittings as a perturbation to the static potential and ignore couplings to decay channels. To first order, then, we have

$$\begin{aligned} M(n^3P_2) &= M_{\text{c.o.g.}} + \Delta M_{\text{SO}} - \frac{1}{10}\Delta M_{\text{tens}}, \\ M(n^3P_1) &= M_{\text{c.o.g.}} - \Delta M_{\text{SO}} + \frac{1}{2}\Delta M_{\text{tens}}, \\ M(n^3P_0) &= M_{\text{c.o.g.}} - 2\Delta M_{\text{SO}} - \Delta M_{\text{tens}}, \\ M(n^1P_1) &= M_{\text{c.o.g.}} - \Delta M^P_{\text{hyp}}, \\ M(n^3S_1) &= \Delta M^S_{\text{hyp}} + M(n^1S_0), \end{aligned} \tag{1}$$

where $M_{\text{c.o.g.}}$ is the mass of the center of gravity of the triplet states.

The wave functions are calculated via the Rayleigh-Ritz-Galerkin method with the Cornell potential [8] and the Indiana potential [9]. The dependence on the choice of potential is small except for the $b\bar{b}$ S-wave states, so we present results using the Cornell potential. The Rayleigh-Ritz-Galerkin method allows analytic Fourier transformation of the wave functions, and we may choose freely between coordinate and momentum space. The difficulties of numerically Fourier transforming the wave functions are avoided.

In coordinate space, the familiar expectation value of an operator ΔH is

$$\langle \Delta H \rangle = \int d^3r \Psi^*(\mathbf{r})\, \Delta H(\mathbf{r}) \Psi(\mathbf{r}), \tag{2}$$

where $\mathbf{r}$ is the relative coordinate of the quark and antiquark. Fourier transforming this expression to momentum space gives the expression [10]

$$\langle \Delta H \rangle = \frac{1}{(2\pi)^6} \int d^3p'\, d^3p\, \tilde{\Psi}^*(\mathbf{p}')\, \Delta\tilde{H}(|\mathbf{p}'-\mathbf{p}|)\, \tilde{\Psi}(\mathbf{p})\,. \tag{3}$$

The angular integrations involved are done analytically in every case.

Perturbative QCD predicts the Fourier transform of the $Q\bar{Q}$ potential, which has been known to $O(\alpha_s^2)$ for some time [4, 5, 11]. We find that the perturbative QCD expectation values are more straightforwardly evaluated in momentum space; however, the long range spin-orbit splitting is more easily calculated in coordinate space.

II. HYPERFINE SPLITTINGS

The hyperfine potential $\Delta\tilde{H}_{\text{hyp}}$ is, in the modified minimal subtraction ($\overline{\text{MS}}$) scheme [4],

$$\Delta\tilde{H}_{\text{hyp}} = \mathbf{s}_1\cdot\mathbf{s}_2\, \frac{32\pi}{9m^2}\, \alpha_s \left\{ 1 + \frac{\alpha_s}{4\pi}\left[\left(-11 + \frac{2}{3}n_f\right) \ln\left(\frac{Q^2}{\mu^2}\right) + \frac{21}{2}\ln\left(\frac{Q^2}{m^2}\right) + \frac{23}{3} - \frac{10}{9}n_f - 3\ln 2 \right] \right\}. \tag{4}$$

Here the momentum transfer $\mathbf{Q} = \frac{1}{2}(\mathbf{p}' - \mathbf{p})$.

The tree-level part of this potential is constant in $\mathbf{Q}$, which corresponds to a δ function in coordinate space and hence will not contribute to the splittings of the P-wave states. Furthermore, in the Gupta-Radford renormalization scheme [5] one would change only the *constant* part of the $O(\alpha_s^2)$ term. This also will not affect the P-wave states. Although we primarily work in the $\overline{\text{MS}}$ scheme we will comment on the effect of scheme dependence where it occurs.

At this point we can motivate our choice of the renormalization scale μ. We would like to have a scale which is related to one of the physical scales of the system we are studying, and at the same time that scale should give small corrections, as the hyperfine splittings are expected to be well-described by perturbative QCD. We see that for $\mu \sim m_q$ both these criteria may be satisfied, as the coefficients of the logarithmic terms in Eq. (4) will then very nearly cancel.

The quantities which depend only on the hyperfine splitting are

$$\begin{aligned} \Delta M^S_{\text{hyp}} &= M(n^3S_1) - M(n^1S_0)\,, \\ \Delta M^P_{\text{hyp}} &= M_{\text{c.o.g.}} - M(n^1P_1)\,. \end{aligned} \tag{5}$$

A. S waves

Performance of the angular integrations for S-wave wave functions yields

$$\begin{aligned} \Delta M^S_{\text{hyp}} = \frac{1}{(2\pi)^6}\frac{16\pi\alpha_s}{9m^2} \int dp'\, dp\, \tilde{\psi}(p')\tilde{\psi}(p) \\ \times \left(p'^2p^2 \left\{ 8\pi + 2\alpha_s\left(\frac{23}{3} - \frac{10}{9}n_f - 3\ln 2\right) - 2\alpha_s\left[\left(-11+\frac{2}{3}n_f\right)\ln(4\mu^2) + \frac{21}{2}\ln(4m^2)\right]\right\} \right. \\ \left. + \alpha_s\left(-\frac{1}{2}+\frac{2}{3}n_f\right)\left\{ \frac{1}{2}p'p(p+p')^2\ln\left[(p+p')^2\right] - 2p'^2p^2 - \frac{1}{2}pp'(p-p')^2\ln\left[(p-p')^2\right]\right\}\right), \end{aligned} \tag{6}$$

TABLE I. Hyperfine splittings.

State	m_q	Experiment	α_s
$c\bar{c}\,1P$	1.2	-0.93 ± 0.23	0.28 ± 0.02
$c\bar{c}\,1S$	1.2	118.1 ± 1.9	0.29 ± 0.01
$c\bar{c}\,2S$	1.2	92.0 ± 5.0	0.30 ± 0.02
$c\bar{c}\,1P$	1.8	-0.93 ± 0.23	0.33 ± 0.02
$c\bar{c}\,1S$	1.8	118.1 ± 1.9	0.34 ± 0.01
$c\bar{c}\,2S$	1.8	92.0 ± 5.0	0.38 ± 0.02

TABLE II. Spin-orbit splittings.

State	m_q	Experiment	α_s
$c\bar{c}\,1P$	1.2	34.92 ± 0.18	0.35 ± 0.01
$b\bar{b}\,1P$	4.6	14.23 ± 0.46	0.26 ± 0.01
$b\bar{b}\,2P$	4.6	9.4 ± 0.2	0.22 ± 0.01
$c\bar{c}\,1P$	1.8	34.92 ± 0.18	0.36 ± 0.01
$b\bar{b}\,1P$	5.2	14.23 ± 0.46	0.26 ± 0.01
$b\bar{b}\,2P$	5.2	9.4 ± 0.2	0.23 ± 0.01

where $\tilde{\psi}(p)$ denotes the radial part of the momentum-space wave function. Figures 1 and 2 show the $c\bar{c}\,1S$ and $2S$ hyperfine splittings as a function of renormalization scale μ for two values of m_c and various values of α_s. These differ slightly from our earlier results [1] due to inaccuracies in our previous determination of the wave functions.

As discussed above, the renormalization scale is chosen to be m_c, which results in small corrections to the tree-level. Table I lists the values of α_s consistent with experiment for this choice [12,13]. Note that for $m_c = 1.8\,\mathrm{GeV}$, the $1S$ and $2S$ states require different values of α_s. This lack of consistency would seem to favor lighter quark masses but could be eliminated by adjusting μ. In the Gupta-Radford scheme [5] we obtain essentially identical results by taking $\mu = 2m_c$. Use of the Indiana potential in calculating the wave functions leads to small increases in the required α_s values. This is due to the less singular behavior of the Indiana potential at small r. Although the effect is small for $c\bar{c}$, it becomes significant for the $b\bar{b}$ S-wave states since those states have larger contributions from high momentum (small r), where the two potentials differ.

B. P waves

The position-space wave functions for the P waves vanish at the origin, leading to two significant simplifications. First, the behavior of the potential at the origin has little effect. Second, after performing the angular integrations the explicit μ dependence which remained in the S wave splittings does not remain in the P wave:

$$\Delta M^P_{\mathrm{hyp}} = -\frac{1}{(2\pi)^6}\frac{8\pi\alpha_s^2}{9m^2}\int dp'dp\tilde{\psi}(p')\tilde{\psi}(p)\left(-\frac{1}{2}+\frac{2}{3}n_f\right)\left\{pp'\left(p^2+p'^2\right)+\frac{1}{4}\left(p^2-p'^2\right)^2\ln\left[\frac{(p-p')^2}{(p+p')^2}\right]\right\}. \tag{7}$$

This independence of renormalization scale makes the prediction of the P-wave splittings much less ambiguous than would otherwise be possible. The P-wave hyperfine splitting depends implicitly on the renormalization scale only through α_s. Figure 3 shows $\Delta M^P_{\mathrm{hyp}}$ for both light and heavy charm-quark masses. For $\alpha_s = 0.3$, we find that $\Delta M^P_{\mathrm{hyp}} = -1.0$ and $-0.78\,\mathrm{MeV}$ for $m_c = 1.2$ and $1.8\,\mathrm{GeV}$, respectively. Included in Table I are the values of α_s which match the recent experimental determination of this splitting [2]. From the table it is clear that once we have chosen α_s to be approximately the same value as required by the $1S$ state, the value $\Delta M^P_{\mathrm{hyp}}$ is almost constant in m_c. That is, for $m_c = 1.2$, $\alpha_s = 0.29$ and $\Delta M^P_{\mathrm{hyp}} = -0.96\,\mathrm{MeV}$, while for $m_c = 1.8$, $\alpha_s = 0.34$ and $\Delta M^P_{\mathrm{hyp}} = -1.00\,\mathrm{MeV}$. We note that this value is rather smaller than previous predictions [4–6].

III. SPIN-ORBIT AND TENSOR SPLITTINGS

The fine structure involves the perturbative QCD result plus an additional spin-orbit term due to confinement. We take the perturbative terms again to be the $O(\alpha_s^2)$ QCD result calculated in the $\overline{\mathrm{MS}}$ scheme [4],

$$\Delta\tilde{H}_{\mathrm{SO}} = \frac{-i\mathbf{s}\cdot\mathbf{p}'\times\mathbf{p}}{Q^2}\frac{2\pi\alpha_s}{m^2}\left\{1+\frac{\alpha_s}{4\pi}\left[\frac{125}{9}-\frac{10}{9}n_f+\left(-11+\frac{2}{3}n_f\right)\ln\left(\frac{Q^2}{\mu^2}\right)+4\ln\left(\frac{Q^2}{m^2}\right)\right]\right\}, \tag{8}$$

$$\Delta\tilde{H}_{\mathrm{tens}} = \frac{\mathbf{s}_1\cdot\mathbf{s}_2Q^2-3\mathbf{s}_1\cdot\mathbf{Q}\mathbf{s}_2\cdot\mathbf{Q}}{Q^2}\frac{16\pi\alpha_s}{9m^2}\left\{1+\frac{\alpha_s}{4\pi}\left[\frac{65}{3}-\frac{10}{9}n_f+\left(-11+\frac{2}{3}n_f\right)\ln\left(\frac{Q^2}{\mu^2}\right)+6\ln\left(\frac{Q^2}{m^2}\right)\right]\right\}. \tag{9}$$

TABLE III. Tensor splittings.

State	m_q	Experiment	α_s
$c\bar{c}\,1P$	1.2	40.34 ± 0.56	0.35 ± 0.01
$b\bar{b}\,1P$	4.6	11.92 ± 0.92	0.27 ± 0.02
$b\bar{b}\,2P$	4.6	9.0 ± 0.4	0.25 ± 0.01
$c\bar{c}\,1P$	1.8	40.34 ± 0.56	0.42 ± 0.01
$b\bar{b}\,1P$	5.2	11.92 ± 0.92	0.28 ± 0.02
$b\bar{b}\,2P$	5.2	9.0 ± 0.4	0.26 ± 0.01

We see immediately that $\mu = m_q$ will not lead to the same cancellations as occurred in the hyperfine case. This is fortuitous as the tree-level calculation, for $\alpha_s \sim 0.3$, gives values much smaller that the experimental splittings; we need large corrections. For the confinement contribution we assume that the confining potential is a pure Lorentz scalar. Working with P waves only, which are insensitive to the short-range behavior of the potential, we once again use the Cornell potential. The additional contribution to the spin-orbit interaction is then [14]

$$\Delta H_{\rm SO}^{\rm conf} = -\frac{a}{2m^2}\frac{\mathbf{L}\cdot\mathbf{S}}{r}, \tag{10}$$

where a is the string tension used in calculating the wave functions. We evaluate this part of the spin-orbit splitting in coordinate space which greatly simplifies the calculation. Carrying out the angular integrations with P-wave wave functions and evaluating the spin-operator expectation values we obtain

TABLE IV. Predicted $b\bar{b}$ hyperfine splittings.

State	$\Delta M_{\rm hyp}$ (MeV)
$b\bar{b}\,1P$	-0.25 ± 0.10
$b\bar{b}\,2P$	-0.21 ± 0.10

$$\begin{aligned}\Delta M_{\rm SO} = {} & \frac{1}{(2\pi)^6}\frac{\pi\alpha_s}{m^2}\int dp'dp\tilde{\psi}(p')\tilde{\psi}(p) \\ & \times\Bigg(\left[8\pi+\frac{44\alpha_s}{9}-2\alpha_s\left(-11+\frac{2}{3}n_f\right)\ln\left(4\mu^2\right)-8\alpha_s\ln\left(4m^2\right)\right] \\ & \times\left\{\frac{1}{2}pp'\left(p^2+p'^2\right)+\frac{1}{8}\left(p^2-p'^2\right)^2\ln\left[\frac{(p-p')^2}{(p+p')^2}\right]\right\} \\ & +2\alpha_s\left(-7+\frac{2}{3}n_f\right)\Bigg\{-\frac{3}{4}pp'\left(p^2+p'^2\right) \\ & -\frac{1}{16}\left(3p^2+2pp'+3p'^2\right)(p-p')^2\ln\left[(p-p')^2\right] \\ & +\frac{1}{16}\left(3p^2-2pp'+3p'^2\right)(p+p')^2\ln\left[(p+p')^2\right] \\ & +\frac{1}{16}\left(p^2-p'^2\right)^2\ln\left[\frac{(p-p')^2}{(p+p')^2}\right]\ln\left[\left(p^2-p'^2\right)^2\right]\Bigg\}\Bigg) \\ & -\int drr^2\psi(r)\frac{a}{2m^2r}\psi(r)\,,\end{aligned} \tag{11}$$

$$\begin{aligned}\Delta M_{\rm tens} = {} & -\frac{1}{(2\pi)^6}\frac{2\pi\alpha_s}{m^2}\int dp'dp\tilde{\psi}(p')\tilde{\psi}(p) \\ & \times\Bigg(\left[\frac{4\pi}{9}+\frac{16\alpha_s}{27}-\frac{\alpha_s}{9}\left(-11+\frac{2}{3}n_f\right)\ln\left(4\mu^2\right)-\frac{2\alpha_s}{3}\ln\left(4m^2\right)\right] \\ & \times\left\{-3pp'\left(p^2+p'^2\right)-\frac{3}{4}\left(p^2-p'^2\right)^2\ln\left[\frac{(p-p')^2}{(p+p')^2}\right]\right\} \\ & +\alpha_s\left(\frac{-5}{9}+\frac{2}{3}n_f\right)\Bigg\{\frac{5}{2}pp'\left(p^2+p'^2\right) \\ & +\frac{1}{8}\left(5p^2-2pp'+5p'^2\right)(p-p')^2\ln\left[(p-p')^2\right] \\ & -\frac{1}{8}\left(5p^2+2pp'+5p'^2\right)(p+p')^2\ln\left[(p+p')^2\right] \\ & -\frac{3}{8}\left(p^2-p'^2\right)^2\ln\left[\frac{(p-p')^2}{(p+p')^2}\right]\ln\left[\left(p^2-p'^2\right)^2\right]\Bigg\}\Bigg)\,.\end{aligned} \tag{12}$$

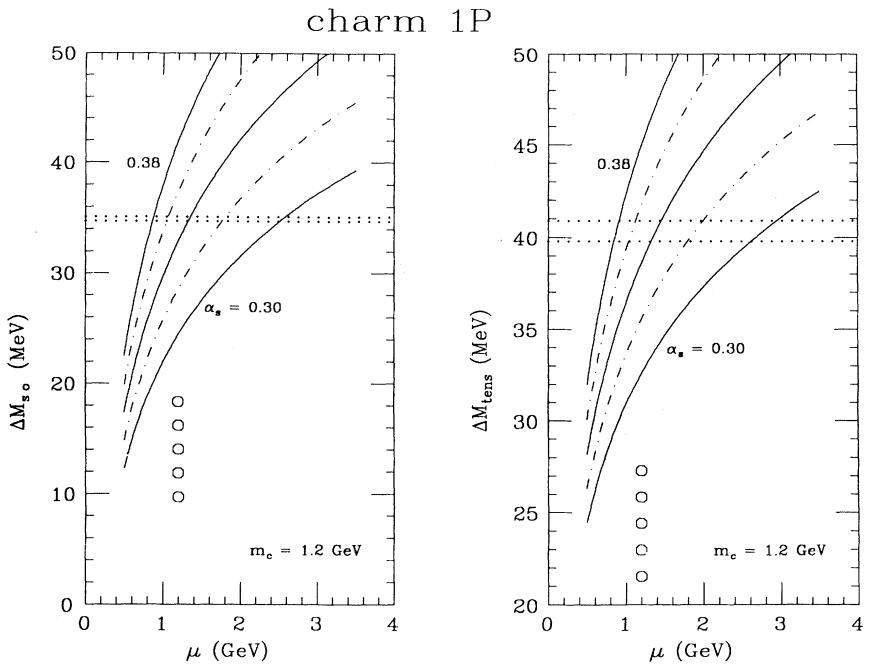

FIG. 4. ΔM_{SO} and ΔM_{tens} in charmonium. The solid and dot-dashed lines show our results for five evenly-spaced choices of α_s. The five large circles are the tree-level results for the same five choices, placed again at $\mu = m_c$. The dotted horizontal lines are the experimental results, as before.

We expect that the spin-orbit and tensor terms should have the same α_s value, as the two interactions have the same $\propto r^{-3}$ behavior when written in coordinate space. Inspection of Tables II and III indicates that this is possible for low quark masses with the exception of the $b\bar{b}2P$ splittings.

In contrast to the hyperfine case, the fine structure involves large corrections to the tree level results. This may be seen clearly from Figs. 4–6. More specific conclusions are unwarranted given the magnitude of the one-loop effects. In particular the drop in the ratio $R = (M_{\chi_2} - M_{\chi_1})/(M_{\chi_1} - M_{\chi_0})$ in the radial excita-

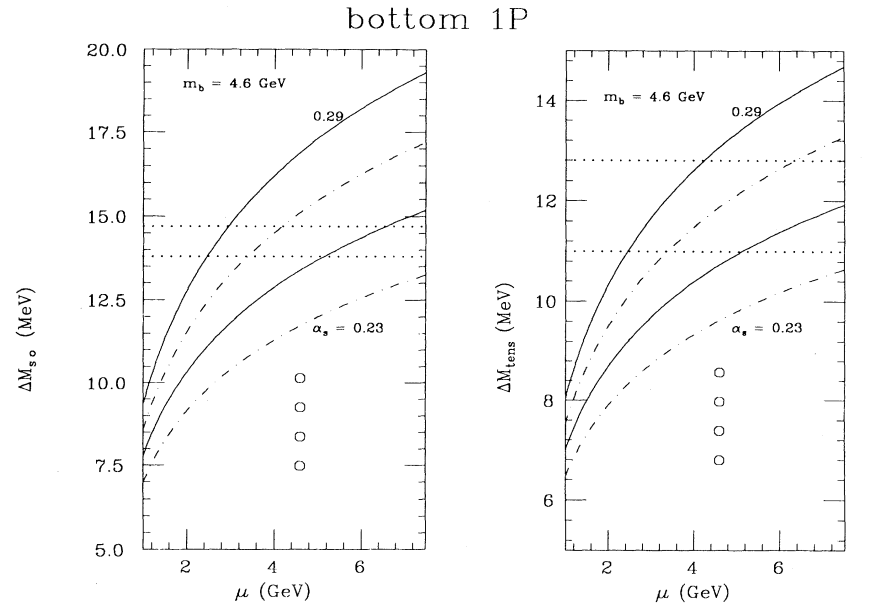

FIG. 5. Similar to Fig. 4, for bottomonium $1P$ states.

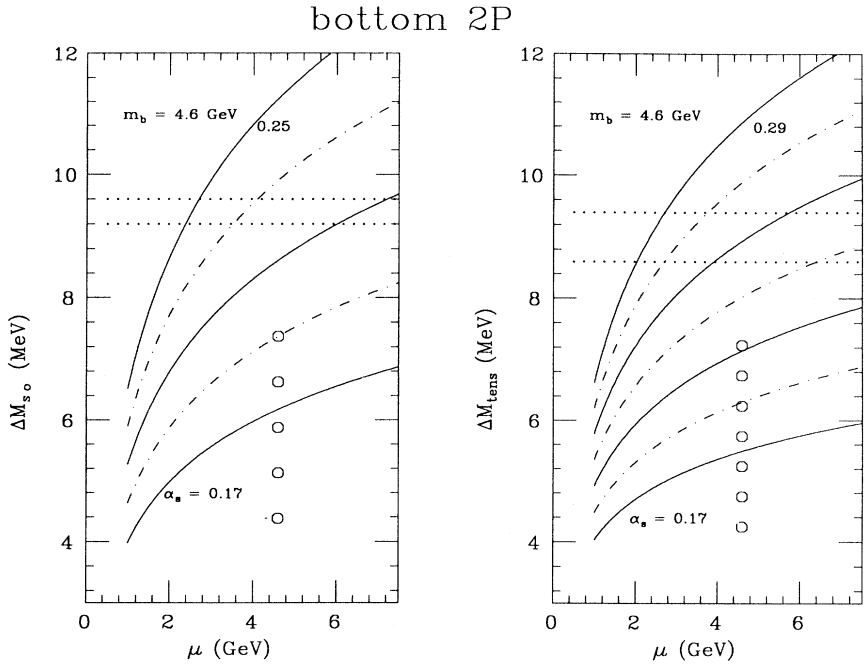

FIG. 6. Similar to Fig. 4, for bottomonium $2P$ states [12].

tion of the χ_b found in recent CESR experiments [13] is still not explained. We point out that the tree-level predictions for spin-orbit and tensor splittings are considerably below the experimental measurements. In each case the one-loop correction is a significant improvement over the tree level and, in fact, provides a reasonable representation of the data.

IV. CONCLUSIONS

While the corrections to the spin-orbit and tensor splittings are large, the corrections to the hyperfine splittings are small and therefore allow reliable predictions of the unmeasured $b\bar{b}$ P-wave singlet states. Similar predictions of the S-wave states would be imprecise because of the

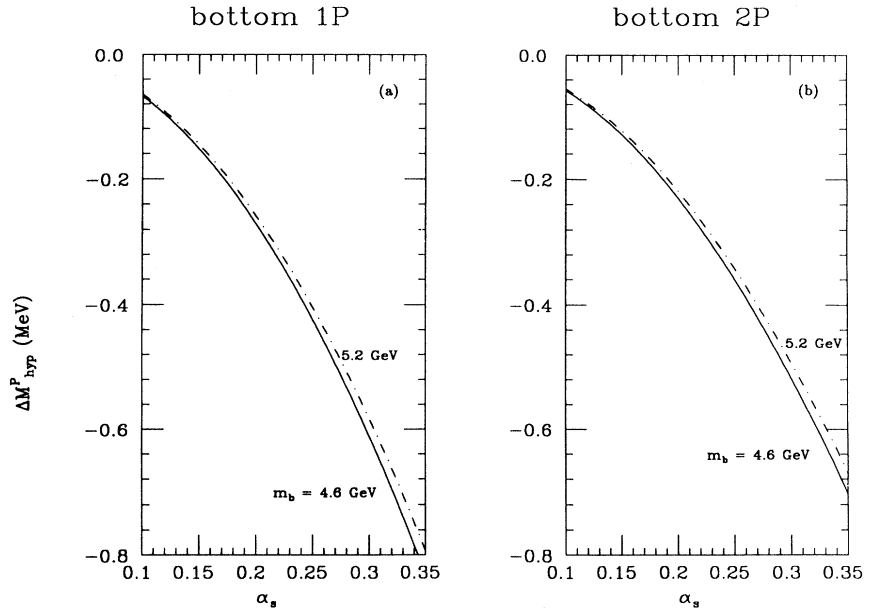

FIG. 7. Similar to Fig. 3, for $b\bar{b}\,1P$ and $2P$.

strong dependence on the form of the potential near the origin, but $\mu = m_b$ will give small corrections regardless of the potential. Our predictions are $\Delta M^P_{\rm hyp}(1P) = -0.25 \pm 0.10\,{\rm MeV}$ and $\Delta M^P_{\rm hyp}(2P) = -0.21 \pm 0.10\,{\rm MeV}$. They are again smaller than previous predictions made with similar calculation schemes, as was the charm $1P$ value [4, 6]. Predictions made with different approaches vary more widely [7]. Table IV lists these predicted splittings. The central values are obtained by the one-loop running from the hyperfine value of $\alpha_s(m_c)$ to $\alpha_s(m_b)$ and it is clear from Fig. 7 that the primary uncertainty is the variation in α_s. We find that QCD provides, at $O(\alpha_s^2)$, a consistent description of all heavy $Q\bar{Q}$ spin splittings.

ACKNOWLEDGMENTS

We would like to thank Kaoru Hagiwara for valuable discussions. This work was funded in part by the University of Wisconsin Research Committee with funds granted by the Wisconsin Alumni Research Foundation, and in part by the U.S. Department of Energy under Contract No. DE-AC02-76ER00881.

[1] F. Halzen, C. Olson, M. G. Olsson, and M. L. Stong, Phys. Lett. B **283**, 379 (1992).
[2] T. A. Armstrong *et al.*, Phys. Rev. Lett. **69**, 2337 (1992).
[3] G. Grunberg, Phys. Lett. **95B**, 70 (1980); **110B**, 501(E) (1982); Phys. Rev. D **29**, 2315 (1984).
[4] J. Pantaleone, S.-H. H. Tye, and Y. J. Ng, Phys. Rev. D **33**, 777 (1986).
[5] S. N. Gupta and S. F. Radford, Phys. Rev. D **24**, 2309 (1981); S. N. Gupta, S. F. Radford, and W. W. Repko, *ibid.* **26**, 3305 (1982); S. N. Gupta and S. F. Radford, *ibid.* **25**, 2690 (1982).
[6] S. N. Gupta, S. F. Radford, and W. W. Repko, Phys. Rev. D **34**, 2201 (1986), J. Pantaleone and S.-H. H. Tye, *ibid.* **37**, 3337 (1988); S. N. Gupta, W. W. Repko, and C. J. Suchyta III, *ibid.* **39**, 874 (1989); D. B. Lichtenberg and R. Potting, *ibid.* **46**, 2150 (1992).
[7] W. Buchmüller, Phys. Lett. **112B**, 479 (1982); J. Stubbe and A. Martin, Phys. Lett. B **271**, 208 (1991); L. P. Fulcher, Phys. Rev. D **42**, 2337 (1990).
[8] S. Jacobs, M. G. Olsson, and C. Suchyta III, Phys. Rev. D **33**, 3338 (1986).
[9] D. B. Lichtenberg, R. Roncaglia, J. G. Wills, E. Predazzi, and M. Rosso, Z. Phys. C **46**, 75 (1990).
[10] The wave functions are normalized to $\int d^3p \left|\tilde{\Psi}(p)\right|^2 = (2\pi)^3$, and the Fourier transformations are $\tilde{f}(\mathbf{p}) = \int d^3r \exp(i\mathbf{p}\cdot\mathbf{r}) f(\mathbf{r})$, and $f(\mathbf{r}) = \int \frac{d^3p}{(2\pi)^3} \exp(-i\mathbf{p}\cdot\mathbf{r}) \tilde{f}(\mathbf{p})$.
[11] W. Buchmüller, Y. J. Ng, and S.-H. H. Tye, Phys. Rev. D **24**, 3003 (1981).
[12] Particle Data Group, K. Hikasa *et al.* Phys. Rev. D **45**, S1 (1992).
[13] M. Narain *et al.*, Phys. Rev. Lett. **66**, 3113 (1991); R. Morrison *et al.*, *ibid.* **67**, 1696 (1991).
[14] T. Appelquist, R. M. Barnett, and K. D. Lane, Annu. Rev. Nucl. Part. Sci. **28**, 387 (1978).